Distribution Agreement

In presenting this thesis as a partial fulfillment of the requirements for a degree from Emory University, I hereby grant to Emory University and its agents the non-exclusive license to archive, make accessible, and display my thesis in whole or in part in all forms of media, now or hereafter now, including display on the World Wide Web. I understand that I may select some access restrictions as part of the online submission of this thesis. I retain all ownership rights to the copyright of the thesis. I also retain the right to use in future works (such as articles or books) all or part of this thesis.

Rui Wu April 9, 2014

Jamming of Static Quasi-2D Emulsions at Various Surfactant Concentrations

by

Rui Wu

Eric R. Weeks
Adviser

Department of Physics

Eric R. Weeks

Adviser

Justin C. Burton

Committee Member

Connie B. Roth

Committee Member

Peter Höyng

Committee Member

2014

Jamming of Static Quasi-2D Emulsions at Various Surfactant Concentrations

By

Rui Wu

Eric R. Weeks

Adviser

An abstract of
a thesis submitted to the Faculty of Emory College of Arts and Sciences
of Emory University in partial fulfillment
of the requirements of the degree of
Bachelor of Sciences with Honors

Department of Physics

2014

Abstract

Jamming of Static Quasi-2D Emulsions at Various Surfactant Concentrations
By Rui Wu

We experimentally investigated the role of surfactants in static oil-in-water emulsions at and above the jamming point. More specifically, we varied the surfactant concentration in the emulsions and studied how the variations impact the critical scaling behaviors of emulsions. The emulsion consists of bidispersed droplets that are ~140 μm in radius on average. The droplets are confined between two parallel glass plates in order to construct a quasi-2D system, which is analogous to other 2D packing systems such as granular disks,[10] except for the following two distinctions. First, our emulsion system is frictionless at static equilibrium, thus the inter-droplet forces are strictly perpendicular to the contact length; second, the droplets in emulsions are highly deformable when compressed, which allows us to easily reach a high area fraction up to ϕ~0.95, which is impossible to achieve for disks. We found that increasing surfactant concentration lowers the jamming point ϕ_c, which we ascribed to the attractive depletion forces induced by micelles formed by surfactants in the emulsion. We studied the critical scaling of coordination number z, and found that the impact of depletion forces is reflected in the behavior of z near the jamming point, but not significant enough over the entire range of ϕ. We also attempted to study inter-droplet forces and bulk pressure of the system, but the empirical law we used to compute forces was developed for a fixed surfactant concentration, therefore unsuitable for our data. Instead, we examined how the average contact length L changes with ϕ, and concluded that in the context of droplet interactions, the influence of depletion forces may be extended to above the jamming point. Our next step will be to re-calibrate the empirical force law and to investigate how it changes with surfactant concentration, which may yield results that are helpful in understanding the role of surfactants in emulsion at a microscopic level.

Jamming of Static Quasi-2D Emulsions at Various Surfactant Concentrations

By

Rui Wu

Eric R. Weeks
Adviser

A thesis submitted to the Faculty of Emory College of Arts and Sciences
of Emory University in partial fulfillment
of the requirements of the degree of
Bachelor of Sciences with Honors

Department of Physics

2014

Acknowledgements

I would like to express my very special thanks to Dr. Eric R. Weeks, for it is he who made this project a reality through his guidance, supervision, and encouragement. Likewise, without the assistance of Dr. Carlos S. Orellana and Xia Hong, in regards to the experimental stage and data analysis stage, my project could not have seen the light of day. I also want to recognize Xin Du and Skanda Vivek for their late night companies in the lab. I would like to express appreciation to Dr. Connie B. Roth, Dr. Justin C. Burton, and Dr. Peter Höyng for being on my honors committee, and *herzlichen Dank* again to Dr. Höyng for this is outside his area of expertise. Last but not least, I would like to thank my roommates, Fanyu Guo and Fangchen Li, for keeping me fed and healthy during the final stage of this project.

Table of Contents

List of Figures and Tables

Introduction

We would like to divide all physical matter into three simple states: solid, liquid and gas, but there are always some materials that cannot be simply classified as just one. At the junction between solid and liquid, there exists materials like toothpaste, sand piles and shaving cream, which can both hold their shape like a solid and flow like a liquid; we refer to these materials as soft matter.

Major categories of soft matter include colloids, glasses, granular systems, foams and emulsions. Colloids are tiny particles suspended in liquid, which includes ink and paint. Glasses here refer to amorphous solids, which are macroscopically hard and resemble crystalline solids, but lack the microscopic structural order of a crystal. This category includes both traditional glasses and plastics. Granular systems consist of discrete solid particles, such as snowflakes, sand grains and coffee beans. Foams, like the foamy beer head, are gas bubbles trapped by liquid. Emulsions are mixtures of two immiscible liquids (usually water and oil), where one exists as small droplets dispersed in the other. Milk, for example, is an emulsion of milk fat and water, and emulsions are also widely used in medicine and cosmetics. In general, soft matter is abundant both in nature and in artificial uses, and plays an important role in many aspects of our life.

The various categories of soft matter may appear intrinsically different, and some may not look “soft” as the name suggests, but they are all composed of constituents that are much smaller than their bulk scales, and they all exhibit an interesting behavior when the concentration of

constituent increases. Think of using flour in the kitchen: if you add a tablespoon of flour to a cup of water, you get a liquid mixture that can thicken your soup or sauce. But if you keep adding flour, the mixture will thicken further and eventually become a bread dough, which behaves more like a plastic, and how hard the dough is will depend on how much flour you add. The qualitative change in properties of the flour-water mixture is due to a process called jamming. When the concentration of a soft matter system rises past the jamming point, the constituent particles begin to fall into mesoscopic non-ordered structures which reduces individual particle motion, and at high concentration the system becomes macroscopically rigid.[14-16] This process is quantifiable: at the jammed state, many of the system's mechanic properties have a power-law dependence on the concentration relative to the jamming point.[5, 7]

Jamming is posited to be a phase transition universal to all soft matters, regardless of the seemingly disparate constituents.[9] In accordance with this principle, my thesis focuses on investigating the characteristics of a static quasi-two-dimensional emulsion and how it can behave like a two-dimensional granular system. The microscopic constituents are oil droplets suspended in water and their concentration is defined as area fraction ϕ, which can be any value between 0 and 1. The droplets are bi-dispersed in size with a radius ratio ~1.55 in

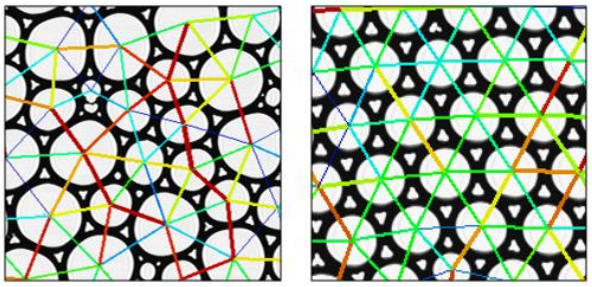

Figure 1. (a) Jamming of bidispersed droplets. (b) A locally crystallized region of monodispersed droplets. In both (a) and (b), the magnitude of inter-droplet forces are marked with a color scale: warmer color represents stronger force. Instead of jamming, monodispersed droplets tend to crystalize and form ordered mesoscopic configurations. The forces between droplets in the crystallized region are more homogeneous and less interesting in the context of our study.

order to prevent crystallization (see Figure 1). Theoretically, when ϕ is at or above the jamming point ϕ_c~0.84,[4, 8, 11] the droplets are in contact with each other and deform under the normal forces at contact.

The jamming transition of emulsions is quantitatively described by critical scaling laws; previous researches, both numerical and experimental, has found that many characteristics of a jammed system have a power law dependence on $(\phi - \phi_c)$.[5, 7, 11] My thesis discusses mainly the scaling law of coordination number, defined as the average number of contacts each droplet has with its neighbors, as well as that of pressure.

Previously in our lab, Desmond *et al*. have done substantial research on the properties of emulsions at a given surface tension.[5] My research extends the previous measurements by varying the surface tension using the surfactant concentration. Surface tension in an emulsion system governs the deformation of droplets, whereas that of solid constituents in granular systems is limited by elasticity of the solid. This provides the emulsion system with an advantage of reaching extremely high area fraction (ϕ~1) with high deformation, which is difficult to achieve in granular systems. In practice, using an emulsion is a more convenient way to experiment on two-dimensional disk systems over a large range of ϕ. However, deformability also limits us to soft-disk systems only. The main focus of my thesis is to what extent we can control the "softness" of the droplets by varying surface tension, and whether such variation affects the critical scaling of the emulsion system.

Procedures

1. Producing droplets

The droplets were produced using a microfluidic method developed by Shah *et al.*[13] We first built a co-flow device consisting of concentric glass capillary tubes as shown in Figure 2 (a). The diameter of the tip of the inner tube is measured to be 38.4 μm and the diameter of the outer tube is approximately 500 μm. To manufacture the tip of the inner tube, we heated up and pulled one end of a capillary tube into a long and thinning hollow fiber, and then used a microforge to melt it up to the desired diameter.

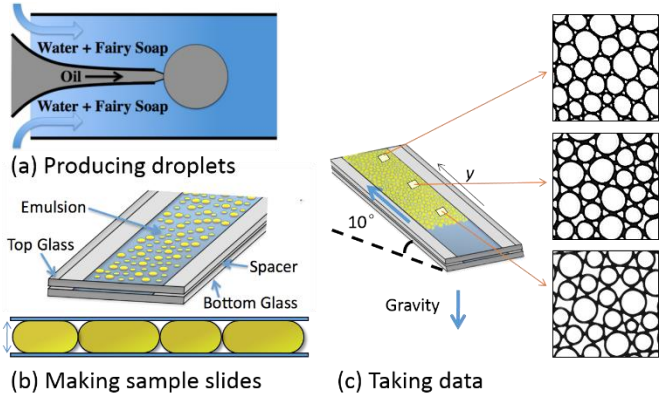

Figure 2. (a) The microfluidic device. Oil accumulates into droplets at the tip and breaks away at a threshold size that is determined by the tip size and flow rates of water and oil. (b) The sample chamber. Droplets are compressed into pancake shapes as shown directly above. (c) The imaging stage. Droplets higher above the incline are compressed by the buoyant weight of droplets below, and are more deformed from the original circular shape.

Mineral oil flows at a constant rate at 0.2 mL/hr through the inner tube, while water flows at a rate that is ~100 times higher than the oil flow rate. The oil will accumulate into a spherical droplet at the inner tip due to surface tension, and the droplet will break away from the tip when it reaches a threshold size. This size is mainly determined by the water and oil flow rates, and the droplets produced under the same set of the flow rates have a fairly low polydispersity in size.[13]

Within a reasonable range, increasing the flow rate of either water or oil will reduce the droplet size. Therefore we were able to use the same microfluidic device to produce droplets of different

sizes: using electronic syringe pumps, we fixed the oil flow rate at 0.2 mL/hr and alternated the water flow rate between 0.4 mL/min and 0.8 mL/min to produce two batches of droplet with a 3D radius ratio of ~1.4. We collected these two batches of droplets in the same container and mixed well to create a large batch of bidispersed droplets.

When producing the droplets, we added Fairy original dish washing soap to water before letting it flow through the device, so that the surfactants in the soap will line the surface of droplets and thus stabilize them. The mass ratio of soap to water here is 1:40 (2.5 g soap to 100.0 g distilled water), which we found to work better with the microfluidic device than other concentrations.

2. Varying surfactant concentration

As stated earlier in this thesis, since surface tension is the major factor that governs many properties of emulsion systems, it is worth investigating how variations in surface tension may affect an emulsion. In our experiments, we changed surface tension of the emulsion system by varying the concentration of surfactant in the system. More specifically, we produced samples of emulsion systems with different soap concentration, ρ_{soap}, to study whether they behave differently.

Initially we performed this variation when producing droplets, and built a separate microfluidic device for each ρ_{soap}. We soon learned that this method has its shortcoming: first, the inner tip of each microfluidic device is not always the same size, as the precision of our pull-and-microforge method is limited; second, since each ρ_{soap} corresponds to a different surface tension, the threshold size at which the droplets break away from the tip also differs.[13] We tried to correct for these effects by adjusting the water and oil flow rates, but the improvement is only marginal as

the electronic pumps we used do not have the precisions that can account for variations at such a microscopic level (see Figure 3). Another problem is that we are interested in a very wide soap concentration range, with the highest ρ_{soap} at 100x of the lowest; however, our microfluidic devices tend to malfunction when ρ_{soap} falls outside an optimal working range. If ρ_{soap} is too low, the droplets are not well stabilized and merge with each other; if ρ_{soap} is too high, the device is often clogged.

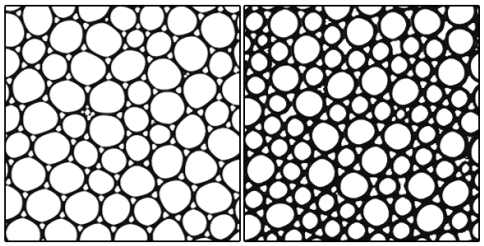

Figure 3. 2D images of droplets produced with 1x (left) and 10x (right) soap concentrations in water, using separate microfluidic devices. The electronic pumps we used to control water flow rate has a precision of 0.1 mL/min, which is not small enough to account for minute variations in surface tension and tip size. As shown here, the deviation of droplet size is still too large after adjusting the flow rates.

We then developed a new method to vary ρ_{soap} in the emulsions: first we produced a mother batch of bidispersed droplets using the same device and choose a ρ_{soap} that works best with the device and the pumps, and then transferred them to water-soap mixtures of a different ρ_{soap}. A droplet is well stabilized by surfactant once it breaks away from the inner tip, and its volume is not likely to change under our experimental settings, hence the transfer does not alter the droplet size. Another advantage of the new method is that since we no longer need multiple microfluidic devices for different ρ_{soap} at the droplet production stage, we can use the same device and same set of water and oil flow rates every time to reduce the polydispersity in droplet size as much as possible.

Using the new method, we produced all droplets at ρ_{soap} = 2.5g/100.0g, and made five daughter batches of droplets with ρ_{soap} at 0.1x, 0.5x, 1.0x, 5.0x and 10x of the original ρ_{soap}. (For convenience, we hereby re-define ρ_{soap} as a dimensionless prefactor that can be multiplied to 2.5g/100.0g to

obtain the true soap concentration; ρ_{soap} of our five droplet batches are thus 0.1, 0.5, 1.0, 5.0 and 10.) When transferring droplets from one water-soap mixture to another, some surfactants might be brought to the new mixture along with the droplet, but this addition is negligible compared to the difference of ρ_{soap} among our samples.

3. Sample chamber and microscopy

To produce a quasi-2D system, we made thin rectangular sample chambers by placing two spacers with thickness ~100 μm between two glass slides, and filled it with droplets. As shown in Figure 2 (b), when droplets enter the sample chamber, they are compressed by the ceiling and the floor of the chamber and made into a pancake shape; the thickness of the sample chamber is small enough compared to its other dimensions and to the smallest droplet diameter, so that the system can be regarded as quasi-2D.[5] Since the large and small droplets are compressed into the same thickness, the quasi-2D radius of the large droplets will increase by a greater amount than that of the small droplets, therefore the radius ratio increases from ~1.4 in 3D to ~1.55 in 2D.

The sample chamber was then set on a 10 °incline under the microscope for 15~20 minutes to let the droplets settle into static equilibrium. The incline helps create a gradient of area fraction through the length of the sample chamber: the droplets higher up the incline must bear the buoyant weight of other droplets below, and therefore they are more compressed and deformed (see Figure 2(c)).

When the entire emulsion system reached static equilibrium, we collected the raw data set of this sample by directly taking images of the droplets. Starting from the very bottom of the droplet

pile, we took a consecutive set of images along the entire length *y* of the sample chamber, each image overlapping with the next at the border by roughly half a droplet. We then stitched these images together in the computer to retrieve the original range of *y*. Our camera takes images of 640x486 pixels with a 1.6x objective lens, which give us a strip at the center of the sample chamber that contains 16-17 droplets in the horizontal range, or 3.9 mm wide. The width of the sample chamber is 6-7 mm, hence our data set represents 55-60% of the entire sample. We have made several samples per ρ_{soap} and chose to present five of them in this thesis; each of our data sets contains roughly 2000 bidispersed droplets.

Results

Once we obtained the stitched image, we divide it into consecutive sampling regions that are defined as $y \pm 5\langle R_o \rangle$. $\langle R_o \rangle$ is the average 3D radius of droplets used to make the same sample, determined from another image taken at low phi. The width of $5\langle R_o \rangle$ gives us enough data points along the entire sample, and enough droplets in each sample region to produce reliable statistics.

We then process the image by sampling region to identify each droplet, as well as the length of contact between them. We do this by dividing the entire sampling region into polygonal section called Voronoi cells (see Figure 4 taken from Ref. 5).[2, 3, 12] We used the radical Voronoi tessellation to ensure that each droplet is entirely contained by its cell, as traditional Voronoi method only considers the center of each

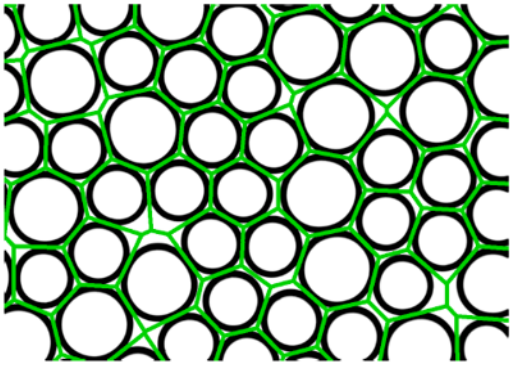

Figure 4. Polygonal Voronoi cells. Each cell contains exactly one droplet and the spaces between droplets are divided between cells.

droplet and ignores its radius, thus often producing cells that are smaller than its droplet. Then we perform a series of algorithms to locate the center and perimeter of each droplet in its own cell, and then compute each contact length between two adjacent droplets. From these preliminary data, we can compute a series of variables, including the area fraction ϕ and the average coordination number z of each sampling region. The detailed methods and algorithms used here are developed by Desmond *et al*.[5]

An important characterizing method for the emulsion system is the statistics of droplet sizes. For our bi-dispersed system, we look at all droplets within the data set and take note of large and small droplet radii, the 2D radii ratio σ_{2D} and the number ratio n_r. The statistics of our five samples are shown in Figure 5 and Table 1. All samples have a small radii spread and the average radii are close to each other; more importantly, σ_{2D} is maintained within a range of 1.55 ±0.05. In the 3D images used to determine $<R_o>$, the droplets have almost identical 3D radius ratio at ~1.4.

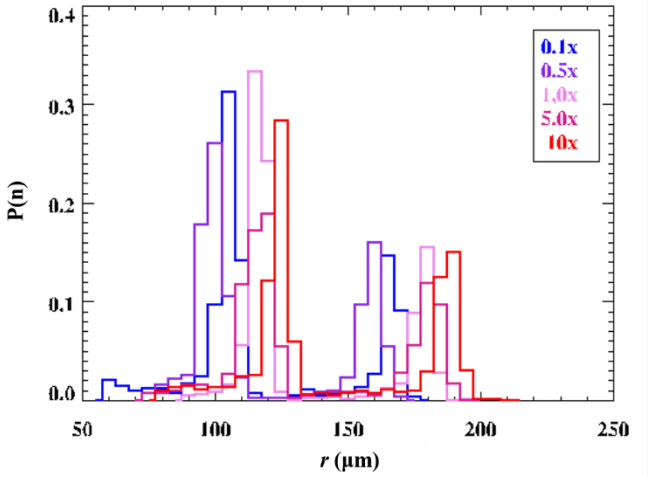

Figure 5. Distribution of droplet radii for all 5 samples. The horizontal displacements of the histograms are not ordered; they are caused by the variations in the thickness of each sample chamber.

Table 1. Droplet size statistics. ρ_{soap} is the mass ratio of soap vs water, which is divided by a prefactor of 2.5g/100.0g; σ_{2D} is the 2D radius ratio and n_r is the number ratio, both are of large vs small droplets.

ρ_{soap}	r_{large} (μm)	r_{small} (μm)	σ_{2D}	n_r
0.1	165	103	1.60	0.46
0.5	160	101	1.58	0.57
1.0	179	118	1.51	0.48
5.0	178	116	1.54	0.56
10	186	122	1.52	0.63

When the droplets are put into the sample chamber, they are compressed into pancakes of the same thickness, and larger droplets deform by a greater faction, thus causing the 2D radius ratio to be higher than the 3D ratio. The slight variations in σ_{2D} is thus more due to the different sample chamber thickness than due to actual dispersion in the droplets. As mentioned in the previous section, our data set represents 55-60% of the entire sample chamber, thus the number ratio n_r here is a close estimation.

1. Identifying the jamming point

We begin describing our emulsion system by finding the gradient of area fraction ϕ and identifying the jamming point ϕ_c. For each sampling region, we first trace the inner perimeter of each droplet and compute the area enclosed by the droplet, A_d, and then compute the area of its corresponding Voronoi cell, A_v; the average area fraction ϕ is then defined as $\phi = \sum_k(A_{d,k})/\sum_k(A_{v,k})$, the overall area ratio of all k droplets in the sampling region versus their Voronoi cells.[5] We compute ϕ of all sampling regions to get $\phi(y)$, which covers the entire y range of our sample chamber.

We define ϕ_c as $\phi(y=0)$, i.e. at the bottom of the droplet pile where the droplets are just entering jamming. However, we cannot directly compute ϕ_c from droplets at $y=0$ alone, because the Voronoi method does not perform well at boundaries of the droplet pile. Instead, we took data points at higher y and extrapolate them to find ϕ at $y=0$. We first tried fitting the entire range of $\phi(y)$ to a power law[5], but we quickly realized that although our power law could fit most of the data nicely, it is prone to large errors at small y, and sometimes gives ridiculous results as ϕ_c (see

Figure 6). Then we tried several different fitting method, and finally settled down to linear fit of the first 10 data points. 10 is approximately the minimum number we can use before the small fluctuation in the data set starts to interfere with linear fitting; the first 10 data points cover less than 1/5 of the entire data set.

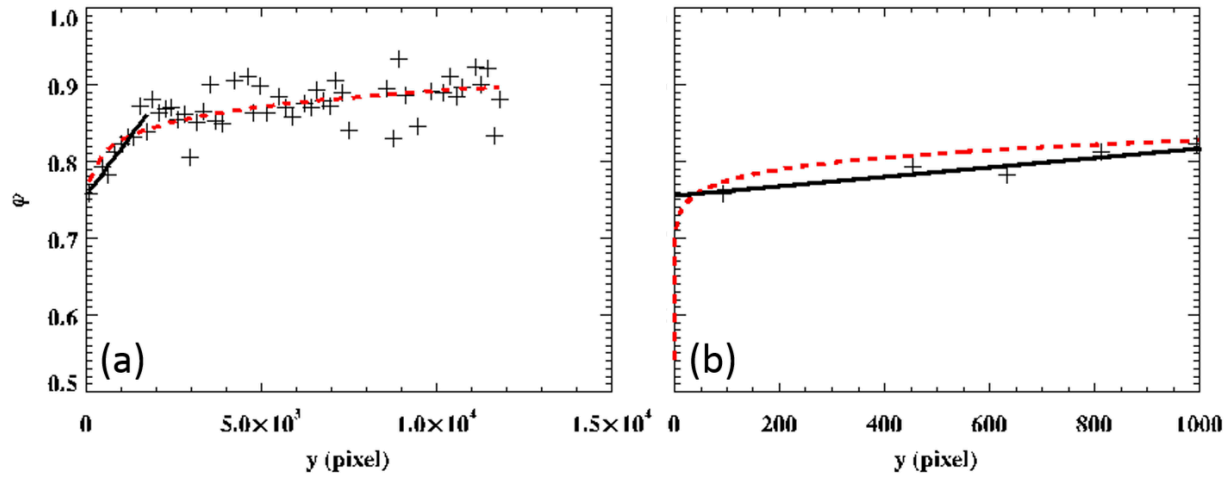

Figure 6. Different fitting methods to determine ϕ_c. (a) The power law fit shown as the dash line fits most parts of the data set nicely. (b) But its behavior changes critically near $y = 0$, giving an impossible value of $\phi_c = 0.46$. The linear fit using only the first few points yields a more reasonable $\phi_c = 0.755$.

Figure 7 shows ϕ_c of our five samples obtained by the linear fit. The experimental $\phi_{c,\mathrm{exp}}$ we obtained is generally lower than the expected $\phi_{c,\mathrm{theory}}$=0.84 from numerical studies, which can be partially attributed to the fact that the boundary of our droplets has a "thickness" of a few pixels, which separates the inner and outer perimeter of

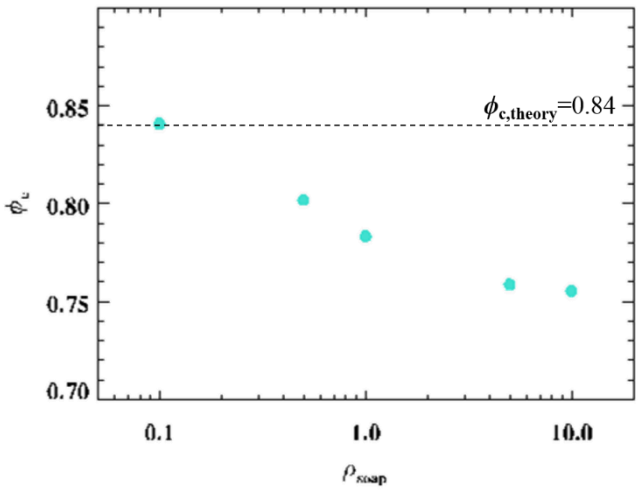

Figure 7. Jamming point of all samples. ϕ_c is determined to be 0.841, 0.802, 0.783, 0.759 and 0.755 for each sample, with the order of increasing concentration.

the droplet; the algorithm used to compute area only considers the inner perimeter, which can give rise to a small systematic error in calculating ϕ. But the main reason here is that $\phi_{c,\text{theory}}$ corresponds to a system in which the interaction between particles are strictly repulsive, and our droplets are observed to have some adhesive properties, hence they could stick to each other and enter jamming well before ϕ reaches 0.84.

The apparent adhesiveness of droplets is most likely due to the presence of micelles in the soapy water we used to produce the droplets. Micelles are tiny balls of surfactant molecules formed in water; each surfactant molecule has its hydrophilic head on the outside of the ball that is in contact with water, and its hydrophobic tail on the inside of the ball, away from water. Micelles only form at and above the critical micelle concentration (CMC); when we are producing droplets, the soapy water must at least reach CMC so as to have enough surfactant molecules lining up the droplet perimeter (a water-oil interface) and stabilizing them, therefore we can be sure that our samples are above CMC and micelles are present.

Since micelles are formed by only a few molecules, it is tiny compared to the droplets. Due to Brownian motion, a droplet is frequently bumped into by micelles; usually these small collisions come from all directions and cancel each other. But when two droplets get close enough that a micelle cannot be squeezed in between them, they are pushed together by micelles bumping from other directions (see Figure 8). The single layer of surfactants on the droplets prevents them from combining, and thus the droplets appear to stick to each other. This effective force that pushes the droplets is called the depletion force.

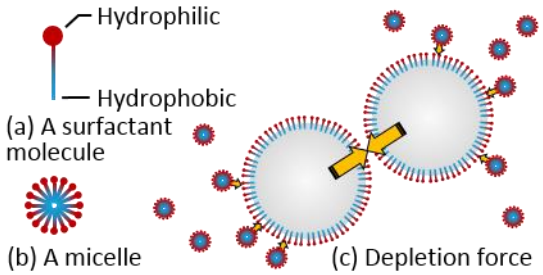

Figure 9. Surfactants, micelles and depletion force (objects in this figure are not to scale). Micelles are formed by a cluster of surfactant molecules with their hydrophobic tails at the center and hydrophilic heads outward. A lone droplet will have micelles bumping into it from all directions; but when two droplets are less than one micelle diameter from the surface of each other, there will be no micelle in the space between them, and the micelles bumping into their rear will effectively push the two droplets together.

The presence of micelles can also explain why ϕ_c decreases with increasing surfactant concentration. At higher concentrations, there are more micelles bumping into the droplets, hence the droplets appear "stickier" than at lower concentrations. Now, in the microscopic context, we define jamming as a state at which the droplets can no longer move freely and do Brownian motion; it does not have to be caused by increasing ϕ. If droplets are sticky due to high surfactant concentration, even at low ϕ they will tend to adhere to each other upon contact, effectively ceasing from individual motion and beginning to jam. In an extreme case shown in Figure 9, surfactant concentration is more than 10x CMC, making the droplets highly adhesive, and the system enters jamming at ϕ ~0.5.

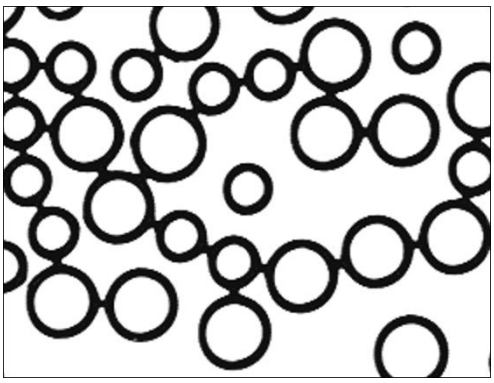

Figure 8. Extremely sticky droplets. When the droplets are highly adhesive, the system enters jamming through the process of droplets sticking to each other, rather than through random close packing. Note that jamming is defined as the state at which the droplets cease from individual motion, thus a jammed system is not necessarily closely packed.

2. Critical scaling

Now that we have ϕ_c for each concentration, we begin investigating the critical scaling of our emulsion systems. The first critical scaling we study is the coordination number *z*, which is defined as the number of contacts each droplet has with all of its neighbors. In simulations of 2D

frictionless disks, z_c=4, which means the droplet receives just enough contact forces from left, right, up and down to keep it in static equilibrium.[6, 7, 11] As ϕ increases, the droplets begin to push into the space between each other and more contacts are made. Here we talk about the average z in our $y \pm 5\langle R_o \rangle$ sampling region as a function of ϕ of the sampling region. The theoretically proposed power law for z is as follows:[7]

$$z - z_c = A_z \cdot (\phi - \phi_c)^{\beta_z},$$

where A_z and β_z are dimensionless fitting parameters. In previous numerical and experimental studies of binary systems, A_z ranges from 3.2 to 4.02, while β_z remains at ~0.5.[6] z_c is the

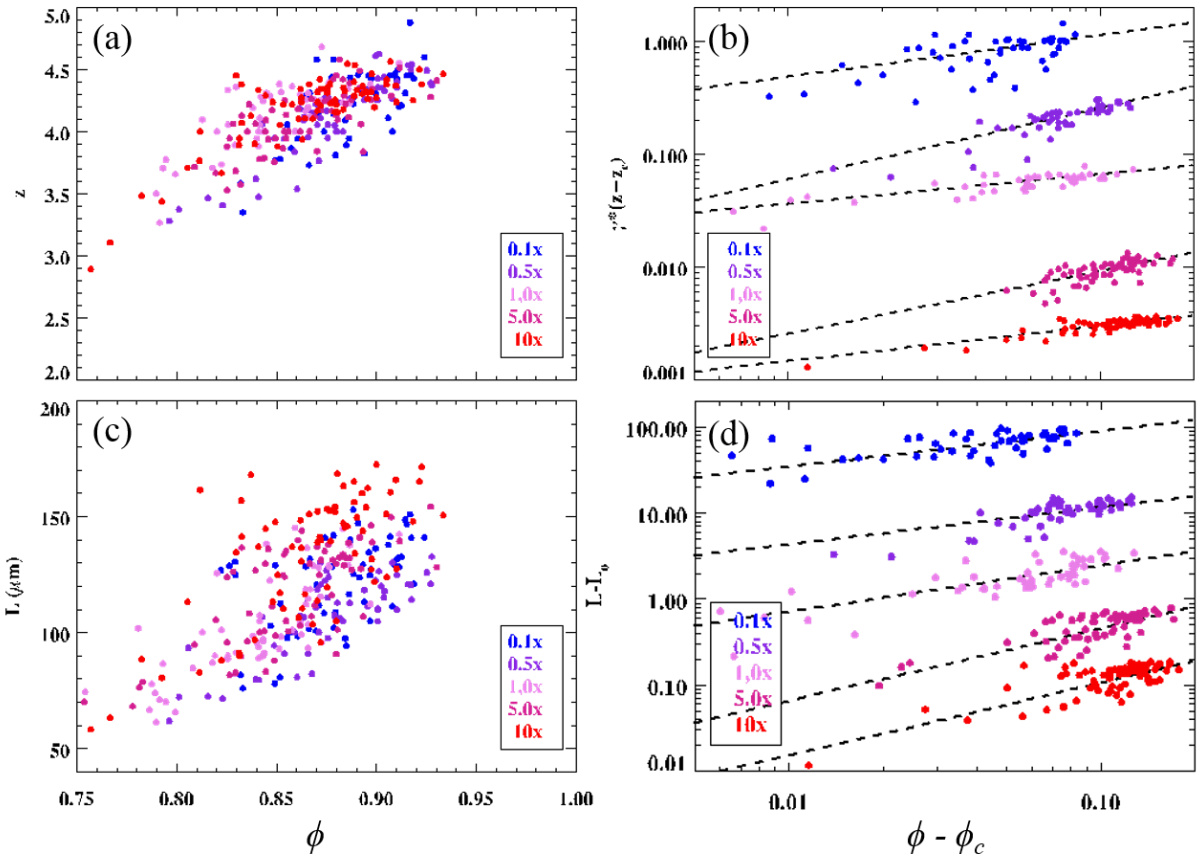

Figure 10. Scatter plots and fit lines for critical scaling of z (above) and L (below); the legend is shown in terms of ρ_{soap}. In (a) and (c), data from all five samples are plotter together; in (b) and (d) they are separated by multiplying a prefactor of γ = 1, 5^{-1}, 5^{-2}, 5^{-3} and 5^{-4} to the original data set.

coordination number that corresponds to the jamming point ϕ_c. Data sets and fit lines of each sample can be found in Figure 10 (a) (b).

Table 2 (a) and Figure 11 shows the fitting parameters of all five concentrations. A_z and β_z show some fluctuation, but are still in the vicinity of their expected values. z_c generally decreases with ρ_{soap}; since z_c directly reflects the system's behavior at ϕ_c, the ranking of z_c is due to the same reason: micelles and depletion force, as we have discussed in the previous section. More specifically, the adhesiveness of droplets allow them to enter jamming by sticking to each other rather than forming close packing, and this gives rise to low z_c. This effect strengthens with increasing ρ_{soap}, and thus causing z_c to decrease with it. In the extreme case shown in Figure 9, the system is already jammed at z_c=2, which is even below the theoretical z_c~3 for 2D frictional systems.[1]

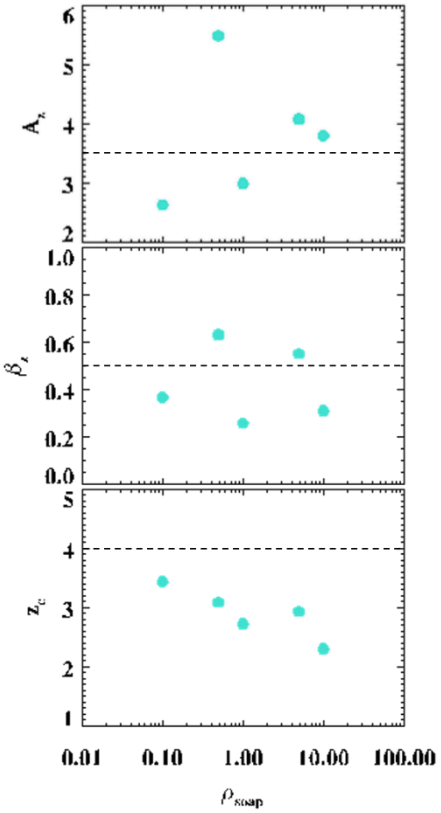

Figure 11. Scatter plots of power law fitting parameters for z vs. ρ_{soap}. While A_z and β_z have greater uncertainties and show fluctuations around their expected values (shown in dashed lines), z_c displays clear trend of decrease with increasing ρ_{soap}. This is due to the same reason that ϕ_c decreases with ρ_{soap}.

We are also interested in the inter-droplet forces, as z only tells us about the geometrical configuration, but not the quantifiable aspect of droplet interactions in jamming. An

Table 2. Power law fitting parameters of the average coordination number z and the average contact length L for each sample.

ρ_{soap}	σ_{2D}	(a) z			(b) L	
		A_z	β_z	z_c	A_L (μm)	β_L
0.1	1.60	2.6	0.37	3.4	232	0.41
0.5	1.58	5.5	0.63	3.1	153	0.42
1.0	1.51	3.0	0.26	2.7	208	0.53
5.0	1.54	4.1	0.55	3.0	393	0.83
10	1.52	3.8	0.31	2.3	460	0.84

empirical force law has been developed to calculate the contact force F based on information of the droplet geometry:[5]

$$F = \alpha_1 \left(R_0 L / r_{ij} \right) + \alpha_2 \left(R_0 L / r_{ij} \right)^2 ,$$

where R_0 is the average 3d radius of large and small droplets combined, L is the contact length, and α_1 and α_2 are constant parameters. r_{ij} here is a measurement of separations between the centers of the two droplets in contact and is defined as $1/r_{ij} = 1/r_i + 1/r_j$.

However, this force law is calibrated to a fixed surfactant concentration of $\rho_{\text{soap}} = 2.0$ (5.0 g soap/100.0 g water),[3] thus the values of α_1 and α_2 are not appropriate to use on our wide range of ρ_{soap}. Recalibrating the force law is very time-consuming, thus we decided to look at contact length L instead as an indicator of the magnitude of inter-droplet forces.

In the raw image of our samples, two neighboring droplets can have a minimum contact length even if they are not jammed. This minimum contact length L_0 is mainly due to the short-range attractive depletion force. In addition, there is a small systematic error due to the limitations in microscope resolution and pixelation. Either way, we need to determine L_0 and deduct it from our raw data.

We used two different methods to determine L_0: the first is doing a preliminary power law fitting with $L - L_c = A \cdot \left(\phi - \phi_c \right)^{\beta}$, and look at the values of L_c, and the second is looking at the

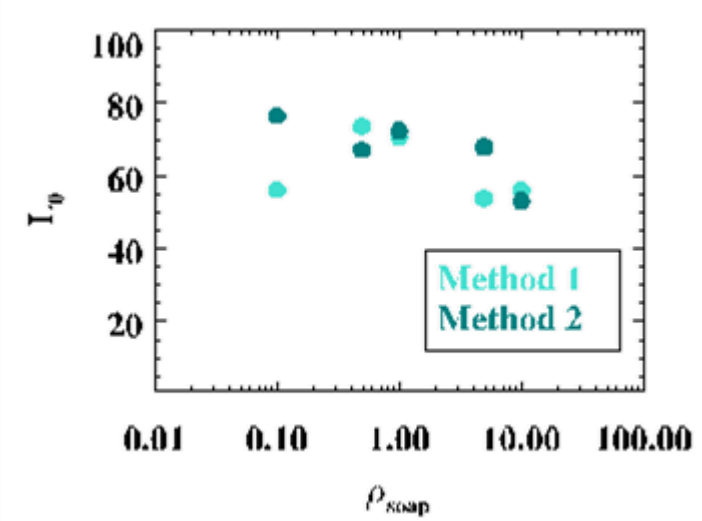

Figure 12. Two methods to determine the minimum contact length L_0. Method 1 shows L_0 determined by the preliminary power law fitting: apart from ρ_{soap} = 0.5 and 1.0 which seems to be outliers, the pattern suggests a common L_0 for all samples. Method 2 shows L_0 determined by manual choice: the descending trend with concentration is not consistent with our depletion force theory, but the variations are small.

raw image of each sample and manually selecting the contact lengths that qualify for identifying L_0. These are contact lengths between droplets with the least deformation (eccentricity~0) at low ϕ. As shown in Figure 12, the first method suggests that we should use the same L_0 for all samples, while the second method produces a descending rank of L_0 with concentration, which seems to contradict with our depletion force theory. Since both methods have their own source of error, we chose to use the average between their results for all samples. We then fit L to the power law

$$L - L_0 = A_L \cdot (\phi - \phi_c)^{\beta_L},$$

where A_L has the same unit as pressure, β_L is the dimensionless power, and L_0 is determined to be 61.3 μm.

The resultant fitting parameters for different concentrations are shown in Table 2 (b) and Figure 13. Unlike in the situation of coordination number z, here all parameters show general ascending trend with

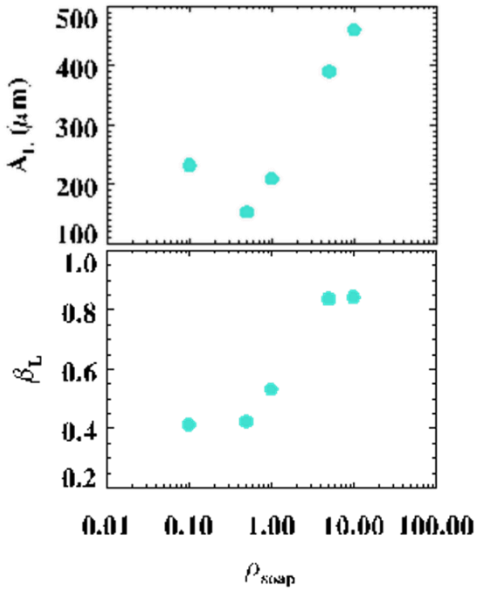

Figure 13. Scatter plots of power law fitting parameters for L vs. ρ_{soap}. Both parameters show general increasing trend, suggesting that the impact of variations in ρ_{soap} may reach beyond the jamming point.

concentration. This may suggest that the impact of depletion force does not stop at the jamming point; however, conclusions can only be drawn with additional information of the alpha constants in the empirical force law.

3. Effect of variations in radius ratio

We have a common concern regarding the accuracy of power law fittings: the radius ratio σ_{2D} of our samples ranges from 1.51 to 1.60, which is a non-trivial variation when characterizing emulsion systems. A previous study done on emulsions at the same surfactant concentration ρ_{soap}=1.0 has shown that fitting parameters tend to drop when σ_{2D} increases: when σ_{2D} changes from 1.42 to 1.52, all fitting parameters drop by a different fraction, averaging at ~10%.[5] In our samples, the two lowest concentrations have σ_{2D} ~ 1.6, hence our power law fitting parameters may need to be amended accordingly.

We did a very coarse adjustment to see if the variation in σ is detrimental to our results. Assuming this change in parameters is universal for all concentrations, we should slightly lower parameters for ρ_{soap} = 0.1 and ρ_{soap} = 0.5 to obtain fitting results that are hypothetically at the same σ. As a rough estimate, the length of each error bar is calculated by calculating the percentage drop of every parameter when σ_{2D} increases from 1.42 to 1.52 (values obtained from previous study done on emulsion with ρ_{soap} = 2.0), and multiplying it to $\sigma_{2D}-1.51$. The 1.51 value is chosen because it is the σ_{2D} of our sample with ρ_{soap} = 1.0, which is closest to ρ_{soap} in the aforementioned previous study. Figure 14 shows these corrections drawn as error bars. For the critical scaling of z, this adjustment reduces fluctuation in β_z, and the concentration ranking in z_c

is conserved; A_z is not improved by much but it does not get worse, either. For pressure, the adjustment flattens but does not completely destroy the ascending trend in either A_L or β_L. We can thus conclude that the variation in σ_{2D} of our samples has some influence on power law fitting, but it does not change what we infer from the fitting results.

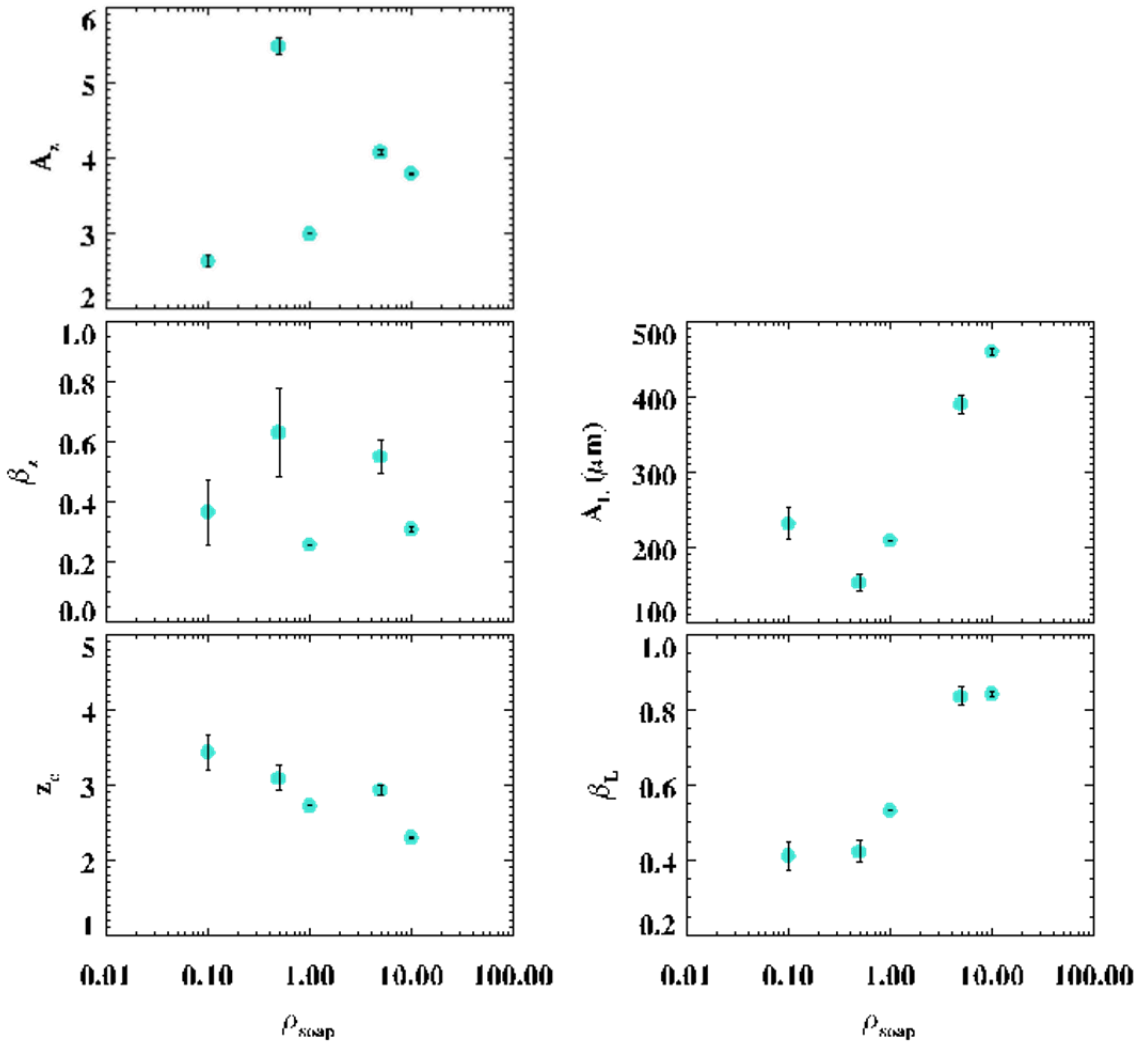

Figure 14. Correction for variations in σ_{2D} plotted as error bars. As a rough estimate, the length of each error bar is calculated by calculating the percentage drop of every parameter when σ_{2D} increases from 1.42 to 1.52 (values obtained from previous study done on emulsion with ρ_{soap} = 2.0), and multiplying it to σ_{2D}−1.51. The 1.51 value is chosen because it is the σ_{2D} of our sample with ρ_{soap} = 1.0, which is closest to ρ_{soap} in the aforementioned previous study. Notice that higher σ_{2D} results in lower parameters; in our samples, the first two concentrations have σ_{2D} that are higher than the rest, hence we should raise the first two data point by the length of their error bar in order to get a hypothetical plot of varying ρ_{soap} and constant σ_{2D}. Although some fitting parameters are more sensitive to variation in σ_{2D} than others, this correction does not change our qualitative findings about the fitting parameters.

Conclusion

We have studied bidispersed quasi-2D water-oil emulsion systems at different surfactant concentrations, ρ_{soap}, and compared the critical scaling of our systems to that of previously studied emulsions at constant surfactant concentration, as well as to that of other 2D binary packing systems in both numerical and experimental research. Our emulsion systems are frictionless and the droplets are highly compressible, which allows us to study them at a wider range of area fraction up to ϕ~0.95. We have developed a method that varies ρ_{soap} of existing emulsions instead of altering it at the stage of producing the emulsions, which reduces deviations in droplet size and size ratio at different surfactant concentrations.

We have found that our emulsions generally enters jamming at a lower ϕ compared to other binary systems such as soft overlapping disks, and attribute this to the depletion forces induced by surfactant micelles in the water which make our droplets slightly adhesive, so that they can jam at low ϕ by sticking to each other. We have also observed that the jamming point ϕ_c drops as surfactant concentration rises, which confirms our reasoning of micelles.

The coordination number z of our system is impacted by variations in ρ_{soap}. We fit the average experimental z and the corresponding ϕ to the power law relationship $z - z_c = A_z \cdot (\phi - \phi_c)^{\beta_z}$, and observed that z_c exhibit similar trend as ϕ_c with increasing ρ_{soap}; this is expected since z_c directly corresponds to z at the jamming point. However, the other fitting parameters do not show clear increasing or decreasing tendencies, which may suggest that variations in surfactant concentration is not dominant besides at the jamming point. It is worth noting that we were able to reach z_c~3,

which corresponds to jamming in 2D frictional systems and may have some implications toward the universality of jamming.

We have also attempted to investigate the inter-droplet contact forces and the pressure determined from these forces, but we were limited by the fact that we rely on an empirical force law determined using emulsions at a fixed ρ_{soap}. Instead, we examined the average contact length L between droplets as an indicator of the magnitude of contact forces, and fit it to the power law $L - L_0 = A_L \cdot (\phi - \phi_c)^{\beta_L}$. We found that unlike that of z, the critical scaling of L is influenced by change in ρ_{soap} even at above the jamming point, as A_L and β_L show ascending trend with increasing ρ_{soap}. However, we cannot yet draw conclusions about inter-droplet forces having the same tendency, since the constant parameters in the force law may change with ρ_{soap} as well. The next step of our project will be to re-calibrate the force law with respect to different ρ_{soap} and investigate how it changes with ρ_{soap}, which may help us understand more about the role of surfactant in emulsions at a microscopic level.

In summary, when we add more surfactants to an emulsion system, the droplets become more adhesive and causes the system to jam at a lower area fraction and coordination number, but it does not significantly alter the system's behavior above the jamming point. We were able to modify the jamming point of emulsion in a wide range to imitate other 2D packing systems that are qualitatively different. Our findings add evidence to the postulate that the phenomenon of jamming is universal in all soft matters, despite their apparent dissimilarities.

References

1 Shlomo Alexander, 'Amorphous Solids: Their Structure, Lattice Dynamics and Elasticity', *Physics Reports,* 296 (1998), 65-236.

2 Franz Aurenhammer, 'Power Diagrams: Properties, Algorithms and Applications', *SIAM Journal on Computing,* 16 (1987), 78-96.

3 Kenneth W Desmond, 'Structure, Dynamics, and Forces of Jammed Systems' (EMORY UNIVERSITY, 2012).

4 Kenneth W Desmond, and Eric R Weeks, 'Random Close Packing of Disks and Spheres in Confined Geometries', *Physical Review E,* 80 (2009), 051305.

5 Kenneth W Desmond, Pearl J Young, Dandan Chen, and Eric R Weeks, 'Experimental Study of Forces between Quasi-Two-Dimensional Emulsion Droplets near Jamming', *Soft Matter,* 9 (2013), 3424-36.

6 DJ Durian, 'Bubble-Scale Model of Foam Mechanics: Melting, Nonlinear Behavior, and Avalanches', *Physical Review E,* 55 (1997), 1739.

7 ———, 'Foam Mechanics at the Bubble Scale', *Physical review letters,* 75 (1995), 4780.

8 Gijs Katgert, and Martin van Hecke, 'Jamming and Geometry of Two-Dimensional Foams', *EPL (Europhysics Letters),* 92 (2010), 34002.

9 Andrea J Liu, and Sidney R Nagel, 'Nonlinear Dynamics: Jamming Is Not Just Cool Any More', *Nature,* 396 (1998), 21-22.

10 Trushant S Majmudar, and Robert P Behringer, 'Contact Force Measurements and Stress-Induced Anisotropy in Granular Materials', *Nature,* 435 (2005), 1079-82.

11 Corey S O'Hern, Stephen A Langer, Andrea J Liu, and Sidney R Nagel, 'Random Packings of Frictionless Particles', *Physical Review Letters,* 88 (2002), 075507.

12 Atsuyuki Okabe, Barry Boots, Kokichi Sugihara, and Sung Nok Chiu, *Spatial Tessellations: Concepts and Applications of Voronoi Diagrams*. Vol. 501 (John Wiley & Sons, 2009).

13 Rhutesh K Shah, Ho Cheung Shum, Amy C Rowat, Daeyeon Lee, Jeremy J Agresti, Andrew S Utada, Liang-Yin Chu, Jin-Woong Kim, Alberto Fernandez-Nieves, and Carlos J Martinez, 'Designer Emulsions Using Microfluidics', *Materials Today,* 11 (2008), 18-27.

14 Alexander ON Siemens, and Martin Van Hecke, 'Jamming: A Simple Introduction', *Physical Review A: Statistical Mechanics and its Applications,* 389 (2010), 4255-64.

15 V Trappe, V Prasad, Luca Cipelletti, PN Segre, and DA Weitz, 'Jamming Phase Diagram for Attractive Particles', *Nature,* 411 (2001), 772-75.

16 M Van Hecke, 'Jamming of Soft Particles: Geometry, Mechanics, Scaling and Isostaticity', *Journal of Physics: Condensed Matter,* 22 (2010), 033101.